

H passivation of Li on Zn-site in ZnO: Positron annihilation spectroscopy and secondary ion mass spectrometry

K. M. Johansen,¹ A. Zubiaga,² F. Tuomisto,² E. V. Monakhov,¹ A. Yu. Kuznetsov,¹ and B. G. Svensson¹¹Centre for Materials Science and Nanotechnology, University of Oslo, N-0318 Oslo, Norway²Department of Applied Physics, Aalto University, P.O. Box 11100, FIN-00076 Aalto, Espoo, Finland

(Received 29 June 2011; published 14 September 2011)

The interaction of hydrogen (H) with lithium (Li) and zinc vacancies (V_{Zn}) in hydrothermally grown n -type zinc oxide (ZnO) has been investigated by positron annihilation spectroscopy (PAS) and secondary ion mass spectrometry. Li on Zn-site (Li_{Zn}) is found to be the dominant trap for migrating H atoms, while the trapping efficiency of V_{Zn} is considerably smaller. After hydrogenation, where the Li_{Zn} acceptor is passivated via formation of neutral $\text{Li}_{\text{Zn}}\text{-H}$ pairs, V_{Zn} occurs as the prime PAS signature and with a concentration similar to that observed in nonhydrogenated Li-poor samples. Despite a low efficiency as an H trap, the apparent concentration of V_{Zn} in Li-poor samples decreases after hydrogenation, as detected by PAS, and evidence for formation of the neutral $V_{\text{Zn}}\text{H}_2$ complex is presented.

DOI: [10.1103/PhysRevB.84.115203](https://doi.org/10.1103/PhysRevB.84.115203)

PACS number(s): 66.30.jp, 81.05.Dz, 78.70.Bj, 71.55.Gs

I. INTRODUCTION

Hydrogen (H) and lithium (Li) are two common impurities in hydrothermally grown (HT) zinc oxide (ZnO), with concentrations typically in the 10^{17} cm^{-3} range,¹ and both elements are electrically active. H can act as a shallow donor²⁻⁴ or indirectly contribute to n -type activity by passivating compensating acceptors.⁵ Li, on the other hand, behaves as an amphoteric impurity, being a donor on an interstitial site (Li_i) and an acceptor on Zn-site (Li_{Zn}).⁵ The relative abundance of Li_i and Li_{Zn} depends on the Fermi-level position and the detailed ZnO stoichiometry.^{6,7} H is a relatively fast diffuser exhibiting an activation energy in the range of 0.8–0.9 eV.^{8,9} Less is known about Li diffusion. However, an early study by Lander¹⁰ suggests an activation energy of 1 eV for migration of Li_i .

In as-grown HT-ZnO the dominant infrared absorption peak, observed at 3577 cm^{-1} , is found to involve both H and Li based upon isotope shift for both elements.^{11,12} Halliburton *et al.*⁵ proposed that this local vibrational mode originates from an OH- Li_{Zn} complex, and they concluded, based on quantification of the absorption line and the strength of the electron paramagnetic resonance (EPR) signal of the Li_{Zn} , that 99% of the Li atoms in their as-grown sample was in the form of such OH-Li complexes. The high apparent thermal stability ($\sim 1250 \text{ }^\circ\text{C}$) of this absorption peak illustrates how efficiently H is trapped by Li_{Zn} , where rapid quenching of the samples to room temperature is needed to avoid retrapping of H upon cooling after high-temperature heat treatment.¹³

However, electrical measurements of similar types of samples^{1,14} showed that the major contribution of Li in as-grown n -type HT-ZnO is in the acceptor state (Li_{Zn}^-) and not in the neutral OH- Li_{Zn} center. By combining secondary ion mass spectrometry (SIMS) with infrared absorption spectroscopy, it has also been found that the absorption strength of the 3577 cm^{-1} line does not scale with the total Li concentration.¹⁵ These results do therefore not support the conclusion that the majority (99%) of Li_{Zn} would be passivated by H in as-grown material via formation of the OH- Li_{Zn} complex.⁵ This is also in line with the recent conclusions of Johansen *et al.*,¹⁶ where the positron annihilation signature of Li_{Zn} has been identified.

In this work, H is deliberately introduced by shallow ion implantation and subsequent annealing (in diffusion), and its interaction with Li_{Zn}^- and V_{Zn}^- is studied by positron annihilation spectroscopy (PAS) and SIMS. Both Li-rich and Li-poor HT ZnO samples have been employed. In the former case, H is found to predominantly passivate the Li_{Zn}^- acceptor leaving V_{Zn} as the main positron trap, while in the latter case an apparent reduction in the concentration of V_{Zn} occurs. V_{Zn} is anticipated to be in a double negative charge state in n -type material,¹⁷ and the results from the Li-poor samples suggest the formation of a neutral $V_{\text{Zn}}\text{H}_2$ complex.

II. METHODOLOGY

Two n -type HT ZnO wafers (labeled A and B) with a size of $10 \times 10 \times 0.5 \text{ mm}^3$ were used in this study and supplied by SPC-Goodwill. A concentration of $2 \times 10^{17} \text{ Li/cm}^3$ was found in wafer A, as measured by SIMS employing a Cameca IMS7f microanalyzer (details about the SIMS analysis can be found in Ref. 16). Wafer B was postgrowth annealed in air at $1500 \text{ }^\circ\text{C}$ (1 h) in order to reduce the Li content, followed by mechanical polishing of the O face to restore the surface smoothness.¹⁴ After polishing, wafer B was further annealed in air at $1100 \text{ }^\circ\text{C}$ (1 h) to minimize the polishing damage in the near-surface region and its influence on PAS Doppler-broadening measurements.¹⁸ The resulting concentration of Li in wafer B, as measured by SIMS, was below $3 \times 10^{15} \text{ cm}^{-3}$; see Fig. 1. The resistivities of wafer A and wafer B (after the postgrowth treatment) were found by four-point probe measurements to be $2 \text{ k}\Omega \text{ cm}$ and $0.6 \text{ }\Omega \text{ cm}$, respectively. One quarter of wafer A and of wafer B (A-2 and B-2) were then implanted on the O face at room temperature (RT) with 35-keV H^- ions to a dose of $1 \times 10^{16} \text{ cm}^{-2}$, while two quarters (A-1 and B-1) were kept as is. The projected range R_p was 265 nm, as estimated by SRIM.¹⁹ A-2 and B-2 were subsequently heat treated at $350 \text{ }^\circ\text{C}$ (30 min) for diffusion of H into the bulk of the samples.⁹

Monoenergetic positrons with energies in the 0.5–38 keV range, giving mean penetration depths of 0.05–2.4 μm , were implanted into the O face of the samples at RT in order to conduct depth-resolved PAS Doppler-broadening

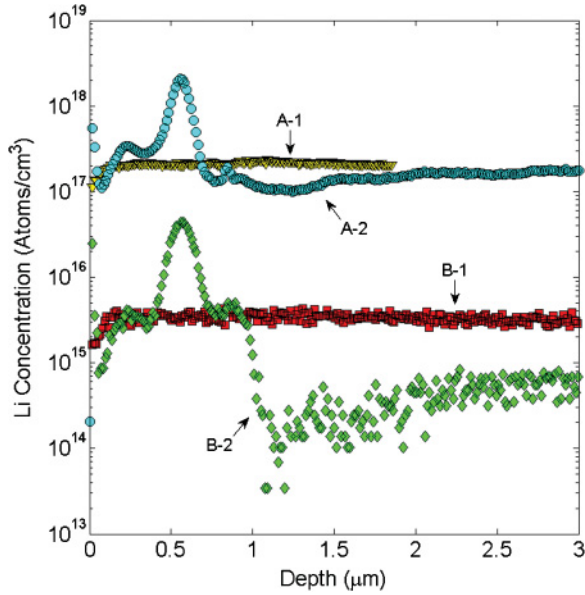


FIG. 1. (Color online) Li concentration vs depth profiles for samples A-1, A-2, B-1, and B-2 as measured by SIMS. The as-grown HT sample A and the post-treated HT sample B contain 2×10^{17} and 3×10^{15} Li/cm³, respectively. After implantation and diffusion, Li has been rearranged in the peak region but still reaches about $1\text{--}2 \times 10^{17}$ cm⁻³ for A-2 and 6×10^{14} cm⁻³ for B-2 at depths exceeding ~ 1 and ~ 2 μm , respectively.

experiments. The Doppler broadening of the annihilation radiation was detected using two Ge detectors with an energy resolution of 1.24 keV at 511 keV. The data were analyzed applying the conventional S and W parameters, defined as the fractions of counts in the central S , $|E - 511 \text{ keV}| \leq 0.8 \text{ keV}$ (corresponding to electron momenta of < 0.4 a.u.), and the wing W , $2.9 \text{ keV} \leq |E - 511 \text{ keV}| \leq 7.4 \text{ keV}$ (1.6–4.0 a.u.), parts of the recorded photon spectrum. Also positron lifetime measurements were undertaken, where a conventional fast-fast coincidence spectrometer with a Gaussian time resolution with full width at half maximum of 250 ps was used.²⁰ During these measurements, the sample and one piece of a reference (high-purity) vapor phase (VP) grown ZnO specimen were sandwiched with a 20- μCi positron source (²²Na deposited on 1.5- μm Al foil). Typically, 2×10^6 annihilation events were collected in each lifetime spectrum, which was analyzed as the sum of exponential decay components convoluted with the Gaussian resolution function of the spectrometer. In the data analysis, materials' specific values for the constant background (including the VP specimen) and annihilation in the source material were accounted for.

Positrons can get trapped and annihilate at neutral and negatively charged open-volume sites in the crystal lattice due to a locally reduced Coulomb repulsion. This increases the positron lifetime and narrows the momentum distribution of annihilating electron-positron (e-p) pairs. These changes can be modeled with *ab initio* methods based on the two-component density functional theory.^{21,22} In positron-annihilation experiments the time-integrated annihilation parameter P_{exp} (e.g., average positron lifetime, S and W parameter) constitutes a weighted sum of the characteristic values of the present positron traps P_i and the crystal lattice P_b ,

$P_{\text{exp}} = \eta_B P_B + \sum_i \eta_i P_i$, with η_B and η_i being the positron annihilation fractions of the lattice and the defect i , respectively. In the case of only one dominant type of vacancy defect, the associated annihilation fraction $\eta_D = \mu_V c_V / (\tau_B - 1 + \mu_V c_V)$, where μ_V is the trapping coefficient of the defect, τ_B is the positron lifetime in the lattice, and $c_V = [V]/N_{\text{at}}$ is the vacancy concentration $[V]$ relative to the atomic density of the lattice (N_{at}).²⁰

III. RESULTS AND DISCUSSION

Figure 1 shows the Li concentration as a function of depth for samples A-1, A-2, B-1, and B-2. A-1 and B-1 have uniform Li concentrations of 2×10^{17} and 3×10^{15} cm⁻³, respectively. However, in A-2 and B-2, Li has redistributed and accumulated in the implantation peak region at the expense of the concentration in the bulk. This process is very similar to that reported by Børseth *et al.*,²³ who found Li to be trapped by implantation-induced vacancy clusters. It should also be noted that, despite the accumulation in the implanted region, the Li concentration in sample A-2 remains close to 2×10^{17} cm⁻³ for depths > 1 μm , while in B-2 it is in the 10^{14} cm⁻³ range for depths at least up to $\sim 3\text{--}4$ μm .

Doppler-broadening experiments were conducted for all the samples, and Fig. 2 shows the S parameter as a function of positron implantation energy with the corresponding mean positron penetration depth depicted on the upper x axis. The peak at ~ 10 keV for samples A-2 and B-2 is related to the damage induced by the implantation of H ($R_p \sim 300$ nm). Our main focus is the region probed by > 25 -keV positrons (depths > 1 μm), and Fig. 3 displays the W parameter versus the S parameter as measured for energies of 25–38 keV. The parameter values are normalized to those of the delocalized

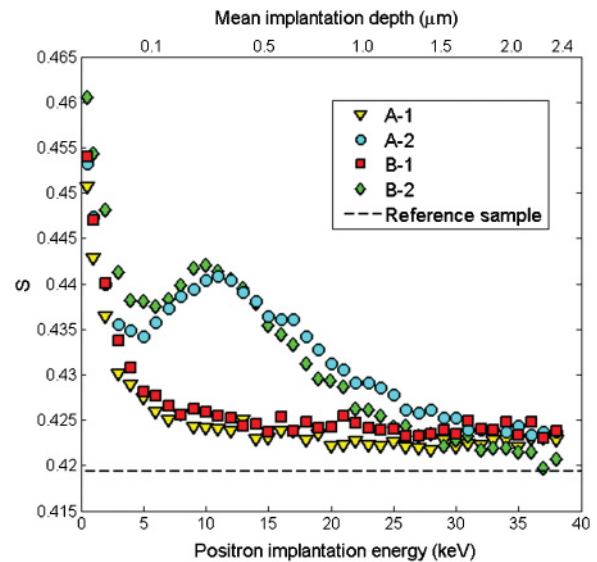


FIG. 2. (Color online) The measured S parameter plotted vs the positron implantation energy (0.5–38 keV) for the A-1, A-2, B-1, and B-2 samples. Positrons implanted with an energy ≤ 5 keV may reach the surface by diffusion and annihilate, leading to the increased S -parameter values observed for low energies. The observed peaks in S -parameter value at ~ 10 keV for samples A-2 and B-2 are caused by the end-of-range defects induced by the H implantation.

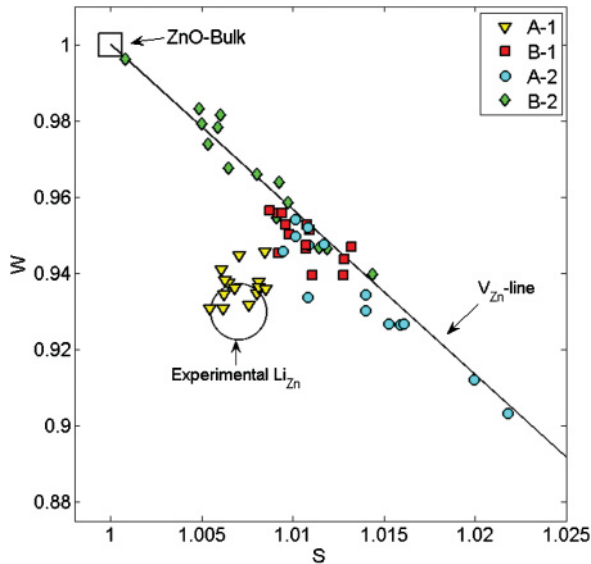


FIG. 3. (Color online) The normalized W parameter vs the S parameter obtained for positron implantation energies ranging from 25 to 38 keV for the Li-rich (A) and the Li-poor (B) HT samples before and after hydrogenation. The black circle represents previously obtained experimental values of the W and S parameters for Li_{Zn} in Li-rich ZnO.^{16,23}

bulk annihilation in the VP-reference specimen, labeled “ZnO-Bulk.” Values for V_{Zn} saturation trapping (not shown) are established from previous studies employing electron and oxygen irradiated samples^{24–26} and taking into account the detector resolution used in the present experiment, giving $S/S_{\text{ref}} = 1.049(3)$ and $W/W_{\text{ref}} = 0.79(1)$.

The line connecting the ZnO-Bulk value with the value for V_{Zn} saturation trapping is referred to as the V_{Zn} line. In samples where the V_{Zn} is the dominant positron trap, the S - and W -parameter values will obey the V_{Zn} line, and the position along the line is determined by the V_{Zn} concentration.²⁴ The black circle in Fig. 3 represents experimental S - and W -parameter values previously found for Li_{Zn} in Li-rich ZnO.^{16,23} The difference found between sample A-1 and B-1 is similar to that reported previously for Li-rich and Li-poor samples¹⁶ and is related to the removal of Li_{Zn} , leaving V_{Zn} as the dominant positron trap.

Interestingly, even though Fig. 1 reveals a Li concentration close to $2 \times 10^{17} \text{ cm}^{-3}$ for sample A-2, the W - and S -parameter values in Fig. 3 follow the V_{Zn} line. This indicates that after hydrogenation Li_{Zn} is not the dominant positron trap, but rather V_{Zn} is.

To gain additional insight into the passivation process, fast positron lifetime measurements were conducted, giving average information over depths up to 100 μm from the sample surface using samples A-1, B-1, A-3, and B-3. Samples A-3 and B-3 were both hydrogenated by heating in a sealed quartz ampoule filled with 0.5 bar of wet ^2H gas for 1 h at 700 $^\circ\text{C}$, expected to give a uniform concentration of ^2H in the 10^{17} cm^{-3} range throughout the samples.⁹ For sample A-1, an average lifetime τ_{ave} of 187 ps is recorded, consistent with that typically found for as-grown (Li-rich) HT ZnO.¹⁶ However, for sample A-3 (Li rich, hydrogenated) τ_{ave} is reduced to 176–177 ps, similar to that for sample B-1 (Li

TABLE I. Estimated apparent V_{Zn} concentration [V_{Zn}] for samples A-2, A-3, B-1, B-2, and B-3 in bulk (beyond the implanted peak). The value for A-1 could not be determined because of the dominant trapping of by Li_{Zn} . The values for B-2 and B-3 are effectively estimated values, not accounting for possible $V_{\text{Zn}}\text{H}_2$ complexes. The vacancy concentrations were determined from the S and W parameters for samples A-2, B-1, and B-2 and from the positron lifetime in A-3 and B-3, using a positron trapping coefficient typical of negative vacancies $\mu_V = 3 \times 10^{15} \text{ s}^{-1}$ (see Ref. 20).

Sample	$[V_{\text{Zn}}]$ (cm^{-3})	Sample	$[V_{\text{Zn}}]$ (cm^{-3})
A-1		B-1	5×10^{16}
A-2	5×10^{16}	B-2	1×10^{16}
A-3	5×10^{16}	B-3	1×10^{16}

poor, not hydrogenated), while for sample B-3 τ_{ave} is even further reduced to 171 ps, close to the bulk value of ~ 170 ps (τ_{B}) for ZnO.²⁵ These results are fully consistent with those obtained by the Doppler-broadening experiments and support a scenario where H primarily interacts with (passivates) the Li_{Zn} acceptor in Li-rich samples and has only a minor effect on the background concentration of V_{Zn} ($\sim 5 \times 10^{16} \text{ cm}^{-3}$). On the other hand, in Li-poor samples V_{Zn} prevails as a major trap for H, and the apparent V_{Zn} concentration deduced by PAS is reduced by a factor of ≥ 5 to $\leq 1 \times 10^{16} \text{ cm}^{-3}$. An overview of the estimated values for the bulk V_{Zn} concentration in samples A-2, A-3, B-1, B-2, and B-3 is given in Table I.

In principle, one could argue that the disappearance of Li_{Zn} as the main positron trap in Li-rich samples after hydrogenation (sample A-2) is not due to passivation but is caused by a change of configuration to Li_i . However, local density functional calculations of formation energies performed by Wardle *et al.*⁶ show that the abundance of Li_{Zn} exceeds that of Li_i by many orders of magnitude in n -type samples prepared under normal conditions. Hence, the formation of Li_i is ruled out as a likely explanation, and in addition, the results in Ref. 6 demonstrate that OH-Li_{Zn} is a highly preferred defect in the presence of hydrogen. Here it should also be mentioned that OH-Li_{Zn} has theoretically been shown to exhibit a similar positron annihilation signature to Li_{Zn} .¹⁶ However, in the neutral charge state of Li_{Zn} the trapping coefficient is significantly reduced compared to the negative charge state due to the decreased Coulomb attraction and relatively small open volume of the defect.

The close resemblance between the concentrations of V_{Zn} in samples B-1 and A-2 indicates that the high temperature anneals at 1500 and 1100 $^\circ\text{C}$ and the hydrogenation process of A-2 have only a minor (if any) influence on the V_{Zn} concentration. Thus, it appears likely that the V_{Zn} concentration in sample A-1 equals that found in A-2 and B-1 (see Table I). This is possibly in contrast to previous results where irradiation-induced V_{Zn} 's were found to anneal out already at 300 $^\circ\text{C}$,²⁵ but it may also indicate that these V_{Zn} 's in the present samples are not isolated, but rather stabilized by other intrinsic defects or impurities. Such a stabilization has already been reported for the Ga vacancy in the GaN system.²⁷

The strong dominance of Li_{Zn} relative to V_{Zn} as a trap for migrating H atoms in wafer A can be partly attributed to its higher concentration ($\sim 2 \times 10^{17} \text{ cm}^{-3}$ versus

$\sim 5 \times 10^{16} \text{ cm}^{-3}$), but not entirely; assuming diffusion-limited reactions and equal capture radii of H by Li_{Zn} and V_{Zn} , only a difference of a factor of ~ 4 in trapping rate is expected, while, experimentally, a factor of ≥ 20 is obtained. On the other hand, if the relative content of Li is sufficiently reduced, V_{Zn} becomes the dominant H trap despite its limited efficiency. This is evidenced by the results for sample B-2, where the Li content is in the low or mid 10^{14} cm^{-3} range for depths less than $\sim 3 \mu\text{m}$ (Fig. 1), while the V_{Zn} content (before hydrogenation) is at least two orders of magnitude higher (sample B-1). A likely reason for the modest H-trapping efficiency of V_{Zn} (versus Li_{Zn}) is that the neutral $\text{V}_{\text{Zn}}\text{H}_2$ complex forms.²⁸ The formation of $\text{V}_{\text{Zn}}\text{H}_2$ requires consecutive trapping of two H atoms, and hence, a low rate of decrease of the apparent V_{Zn} concentration occurs. Further, the formation of the $\text{V}_{\text{Zn}}\text{-H}_2$ complex fully explains the apparent low V_{Zn} concentration in samples B-2 and B-3. The effect of adding two H atoms into the Ga vacancy in GaN (with very similar positron characteristics to the Zn vacancy in ZnO) results in a reduction of the difference between τ_{V} and τ_{B} by 45 ps (from 70 ps).²⁷ A similar lifetime reduction is likely for the $\text{V}_{\text{Zn}}\text{-H}_2$ complex and is enough to explain the decrease of the average lifetime as seen for B-3 as compared to B-1. Similarly, the addition of two H atoms into the vacancy draws the S and W parameters of the vacancy defect much closer to the ZnO bulk value, explaining the apparent low V_{Zn} concentration obtained for B-2. Hence it can be concluded that the hydrogenation

does not truly reduce the Zn vacancy concentration but reduces the open volume in the Zn vacancies by hydrogen filling.

IV. CONCLUSION

In as-grown HT ZnO samples the Li_{Zn} acceptor is found to be efficiently passivated by hydrogen, introduced via diffusion from the O face, and its characteristic PAS signal disappears while forming the neutral OH- Li_{Zn} complex. For V_{Zn} , the opposite holds, and it emerges as the dominant positron trap after the hydrogenation with a concentration similar to that detected in postgrowth-annealed Li-poor HT samples. However, in the latter samples, where the Li content is about two orders of magnitude lower than the V_{Zn} content and Li does not truly compete for H trapping, hydrogenation leads to a decrease in the PAS signal of V_{Zn} . This decrease is presumably due to formation of the neutral $\text{V}_{\text{Zn}}\text{H}_2$ complex, and the apparent V_{Zn} concentration, as detected by PAS, approaches the bulk value of high-purity VP samples ($\leq 1 \times 10^{16} \text{ cm}^{-3}$).

ACKNOWLEDGMENTS

Financial support from the FUNMAT@UiO program and the Norwegian Research Council (NANOMAT and FRINAT programs), NORDFORSK, and the Academy of Finland is gratefully acknowledged.

¹L. Vines, E. V. Monakhov, R. Schifano, W. Mtangi, F. D. Auret, and B. G. Svensson, *J. Appl. Phys.* **107**, 103707 (2010).

²C. G. Van de Walle, *Phys. Rev. Lett.* **85**, 1012 (2000).

³S. F. J. Cox *et al.*, *Phys. Rev. Lett.* **86**, 2601 (2001).

⁴A. Janotti and C. G. Van de Walle, *Nat. Mater.* **6**, 44 (2007).

⁵L. E. Halliburton, L. Wang, L. Bai, N. Y. Garces, N. C. Giles, M. J. Callahan, and B. Wang, *J. Appl. Phys.* **96**, 7168 (2004).

⁶M. G. Wardle, J. P. Goss, and P. R. Briddon, *Phys. Rev. B* **71**, 155205 (2005).

⁷A. Carvalho, A. Alkauskas, A. Pasquarello, A. Tagantsev, and N. Setter, *Phys. B* **404**, 4797 (2009).

⁸D. G. Thomas and J. J. Lander, *J. Chem. Phys.* **25**, 1136 (1956).

⁹K. M. Johansen, J. S. Christensen, E. V. Monakhov, A. Y. Kuznetsov, and B. G. Svensson, *Appl. Phys. Lett.* **93**, 152109 (2008).

¹⁰J. J. Lander, *J. Phys. Chem. Solids* **15**, 324 (1960).

¹¹E. V. Lavrov, *Phys. B* **340-342**, 195 (2003).

¹²G. A. Shi, M. Stavola, and W. B. Fowler, *Phys. Rev. B* **73**, 081201 (2006).

¹³K. M. Johansen, H. Haug, E. Lund, E. V. Monakhov, and B. G. Svensson, *Appl. Phys. Lett.* **97**, 211907 (2010).

¹⁴B. G. Svensson *et al.*, *Mater. Res. Soc. Symp. Proc.* **1035**, L04-01 (2008).

¹⁵K. M. Johansen, H. Haug, Ø. Prytz, P. T. Neuvonen, K. E. Knutsen, L. Vines, E. V. Monakhov, A. Y. Kuznetsov, and B. G. Svensson, *J. Electron. Mater.* **40**, 429 (2011).

¹⁶K. M. Johansen, A. Zubiaga, I. Makkonen, F. Tuomisto, P. T. Neuvonen, K. E. Knutsen, E. V. Monakhov, A. Y. Kuznetsov, and B. G. Svensson, *Phys. Rev. B* **83**, 245208 (2011).

¹⁷A. Janotti and C. G. Van de Walle, *J. Cryst. Growth* **287**, 58 (2006).

¹⁸F. A. Selim, M. H. Weber, D. Solodovnikov, and K. G. Lynn, *Phys. Rev. Lett.* **99**, 085502 (2007).

¹⁹J. Ziegler, *SRIM—The Stopping and Range of Ions in Matter, version SRIM-2006, computer code.*

²⁰K. Saarinen, P. Hautojärvi, and C. Corbel, in *Identification of Defects in Semiconductors*, edited by M. Stavola, Semiconductors and Semimetals, Vol. 51A (Academic, San Diego, 1998), pp. 209–285.

²¹M. J. Puska and R. Nieminen, *Rev. Mod. Phys.* **66**, 841 (1994).

²²C. Rauch, I. Makkonen, and F. Tuomisto, *Phys. Rev. B* (to be published).

²³T. M. Børseth, F. Tuomisto, J. S. Christensen, W. Skorupa, E. V. Monakhov, B. G. Svensson, and A. Y. Kuznetsov, *Phys. Rev. B* **74**, 161202 (2006).

²⁴F. Tuomisto, V. Ranki, K. Saarinen, and D. C. Look, *Phys. Rev. Lett.* **91**, 205502 (2003).

²⁵F. Tuomisto, K. Saarinen, D. C. Look, and G. C. Farlow, *Phys. Rev. B* **72**, 085206 (2005).

²⁶A. Zubiaga, F. Tuomisto, V. A. Coleman, H. H. Tan, C. Jagadish, K. Koike, S. Sasa, M. Inoue, and M. Yano, *Phys. Rev. B* **78**, 035125 (2008).

²⁷S. Hautakangas, I. Makkonen, V. Ranki, M. J. Puska, K. Saarinen, X. Xu, and D. C. Look, *Phys. Rev. B* **73**, 193301 (2006).

²⁸E. V. Lavrov, J. Weber, F. Börrnert, C. G. Van de Walle, and R. Helbig, *Phys. Rev. B* **66**, 165205 (2002).